The Canadian Mineralogist
Vol. 47, pp. 297-302 (2009)
DOI: 10.3749/canmin.47.2.297

THE CRYSTAL CHEMISTRY OF THE KORNERUPINE–PRISMATINE SERIES. IV. COMPLETE CHEMICAL FORMULAE FROM ELECTRON-MICROPROBE DATA AND X-RAY POWDER DIFFRACTION

MARK A. COOPER AND FRANK C. HAWTHORNE§

Department of Geological Sciences, University of Manitoba, Winnipeg, Manitoba R3T 2N2, Canada

ABSTRACT

A procedure is developed whereby complete chemical formulae and chemical compositions of kornerupine may be derived from electron-microprobe data and unit-cell dimensions. The boron content (as B in *apfu*) can be expressed as a linear function of the *a* and *c* cell parameters and the Al_2O_3 and FeO contents (as wt.% oxide). The content of ferric iron (as Fe^{3+} in *apfu*) can be expressed as a linear function of the B content (as B *apfu*) and the Al_2O_3 and FeO contents (as wt.% oxide). The hydrogen content (in H *apfu*) can be expressed as 1 – F (*apfu*). Standard errors of estimates for B and Fe^{3+} are both 0.05 *apfu*.

Keywords: kornerupine, chemical formula, chemical composition.

SOMMAIRE

Nous avons développé une procédure permettant d'obtenir une formule chimique et une composition chimique complètes d'un échantillon de kornérupine à partir de données acquises avec une microsonde électronique et les paramètres réticulaires. On peut exprimer la teneur en bore, en atomes par formule unitaire, *apfu*, par une fonction linéaire des paramètres *a* et *c*, et des teneurs en Al_2O_3 et FeO (en %, poids). On peut exprimer la teneur en fer ferrique par une fonction linéaire de la teneur en B (en *apfu*) et des teneurs en Al_2O_3 et FeO (en %, poids). La teneur en hydrogène (en *apfu*) est équivalente à 1 – F. Les erreurs standards associées aux valeurs estimées de B et de Fe^{3+} sont environ 0.05 *apfu*.

(Traduit par la Rédaction)

Mots-clés: kornérupine, formule chimique, composition chimique.

INTRODUCTION

Kornerupine, (□,Mg,Fe) $(Al,Mg,Fe)_9$ $(Si,Al,B)_5$ O_{21} (OH,F), occurs in high-grade metamorphic rocks, especially those rich in Mg and Fe, and yet there is very little complete chemical information on this mineral compared with other rock-forming silicate minerals. This lack of information is a result of the difficulty in completely analyzing kornerupine. As kornerupine contains essential B in variable quantities, together with Al in tetrahedral and octahedral coordination, and significant and variable amounts of vacancy at one site (*X*), omission of B from the analytical procedure prevents calculation of a mineral formula. Most recent work on the composition of kornerupine (*e.g.*, Grew *et al.* 1990, Hawthorne *et al.* 1995) has involved the use of an ion microprobe to determine B content. Although this approach does overcome the major problem in deriving kornerupine formulae, there are three additional problems: (1) the issue of Fe^{3+}:Fe^{2+} ratio is not addressed, (2) H is not determined, and (3) access to an ion microprobe is a problem for many scientists.

Here, we take a different approach to the chemical analysis of kornerupine: we use well-established crystal-chemical correlations and X-ray powder-diffraction to derive compositional parameters that cannot be measured by electron-microprobe analysis. For kornerupine, Cooper *et al.* (2009a, b) and Hawthorne *et al.* (1995) have established very well-developed correlations between B content, H content and Fe^{3+} content, and the unit-cell dimensions and chemical parameters determined by electron-microprobe analysis. These are used to derive the complete chemical formula (and chemical composition) of kornerupine.

§ *E-mail address*: frank_hawthorne@umanitoba.ca

Derivation of H, B and Fe^{3+}

Hydrogen

Cooper *et al.* (2009b) showed that OH + F = 1.0 *apfu* in kornerupine. As F is measured by electron-microprobe analysis, H may be calculated as H = (1.0 – F) *apfu*.

Boron

The B content of kornerupine varies in the range 0.0–0.9 *apfu* (0.0–4.2 wt.% B_2O_3), and the results of Cooper *et al.* (2009a) show that B is completely ordered at the *T*(3) site. As B ($^{[4]}r$ = 0.11 Å) is much smaller than Si ($^{[4]}r$ = 0.26 Å) and Al ($^{[4]}r$ = 0.39 Å), incorporation of B at *T*(3) produces significant dimensional changes within the kornerupine structure. Figure 1 shows the adjustments of the *T*(2)–*T*(3)–*T*(2) trimer in response to various B contents at *T*(3). In particular, the O(7)–O(7) and O(8)–O(8) edges contract significantly with incorporation of B at *T*(3). For K40 (B = 0.016 *apfu*) and K41 (B = 0.880 *apfu*), the values are as follows: O(7)–O(7): 2.786 and 2.464 Å; O(8)–O(8): 2.730 and 2.513 Å. The O(7)–O(7) and O(8)–O(8) edges of the *T*(3) tetrahedron lie along [100] and [001], respectively, and hence the *a* and *c* cell-dimensions should be sensitive to variations in the B content of the crystal.

Hawthorne *et al.* (2009) show that many chemical parameters in kornerupine correlate with B content. Thus the major-element composition derived from the electron-microprobe analysis can serve to further define the B content of the crystal. Multiple linear regression with B as the dependent variable and *a*, *c*, Al_2O_3 and FeO* *apfu* (FeO* = total Fe expressed as FeO) as independent variables gives an excellent correlation (r^2 = 0.989; equation 1, Table 1); Figure 2 shows the agreement between the corresponding observed (B_{SREF}) and calculated (B_S) values.

Iron

The Fe^{2+} content of kornerupine ranges from 0.00 to 1.29 *apfu* (0.00 to 12.09 wt.% FeO) and the Fe^{3+} content from 0.00 to 0.35 *apfu* (0.00 to 3.63 wt.% Fe_2O_3). Ferrous iron is disordered over two octahedra [*M*(1), *M*(2)] and one [8]-coordinated *X*-site, and all Fe^{3+} is ordered at the *M*(4) site (Cooper *et al.* 2009a). Multiple regression with Fe^{3+} as the dependent variable and B_S, Al_2O_3 and FeO* as independent variables (Equation 4, Table 1) gives a good correlation (r^2 = 0.952) for kornerupine samples with appreciable Fe^{3+} content (*i.e.*, > 0.03 *apfu* Fe^{3+}); Figure 3 shows the agreement between the corresponding observed (Fe^{3+}_{SREF}) and calculated (Fe^{3+}_S) values. There is significantly more dispersion for the low-Fe^{3+} crystals in Figure 3 than for crystals with Fe^{3+} > 0.03 *apfu*, but the reason for this is not clear. Possibly where Fe^{3+} = 0, there is accumulated strain in the structure, leading to deviation from the relations developed above. Samples K3 and K33 are

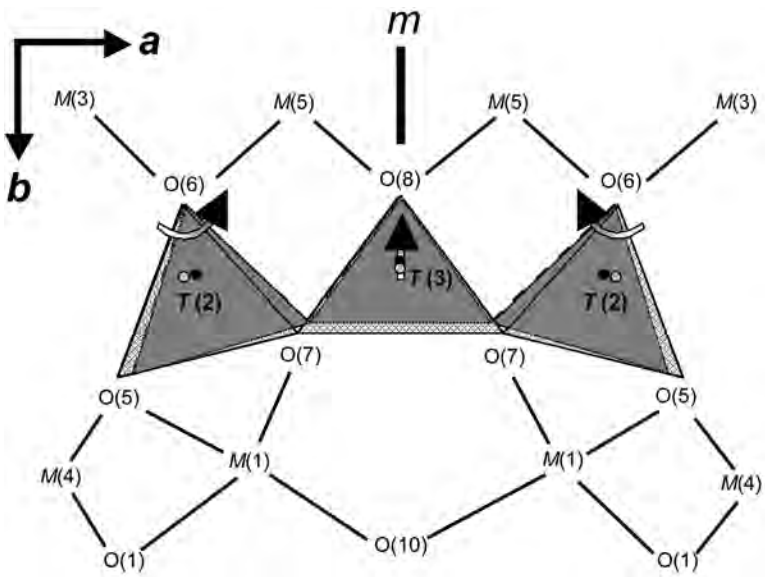

FIG. 1. Adjustments of the *T*(2)–*T*(3)–*T*(2) trimeric cluster in kornerupine as a function of B content. Projected onto (001). Low-B: tetrahedra are shaded light grey, *T* sites are grey circles; high-B: tetrahedra are shaded dark grey, *T* sites are black circles.

from Andhra Pradesh, India, and plot somewhat off the relation in Figure 3 for unknown reasons, and were excluded in the final regression analysis.

Cell parameters

For all 47 samples of kornerupine refined by Cooper *et al*. (2009a), the B and Fe^{3+} content can be calculated to within about ±0.05 *apfu* of the values determined by SREF, using the Al_2O_3 and FeO* contents and the *a* and *c* cell-parameters [equations (1) and (4), Table 1]. Thus the calculated B and Fe^{3+} contents are both dependent upon the cell parameters. The cell parameters used in the regression equations of Table 1 are those determined by single-crystal X-ray diffraction. As many mineralogists do not have the necessary instrumentation available, we also examined the effect of using cell dimensions determined by powder diffraction.

X-Ray Powder-Diffraction Study

Nine small (3–8 mg) clean separates of kornerupine were ground to a fine powder with an internal standard (10% by weight NBS 640b); X-ray-diffraction data were collected using an automated Philips PW1710 goniometer fitted with 1° slits in step-scan mode (0.02° steps, 5 s / step) from 6 to 66° 2θ. Powdered samples were placed on a quartz plate to reduce the background signal. The Jade software package (v. 6.5) was used to process the powder data. Background was modeled by a cubic spline and then removed. Peak positions were determined using refined peak profiles ($K_{\alpha 2}$ modeled) and scaled against the internal standard for eleven well-resolved peaks of kornerupine lying between 26 and 62° 2θ. The eleven peaks chosen (Table 2) were the strongest and best resolved on *all* diffractograms. In addition, the powder patterns calculated from the single-crystal refinements show that these eleven peaks

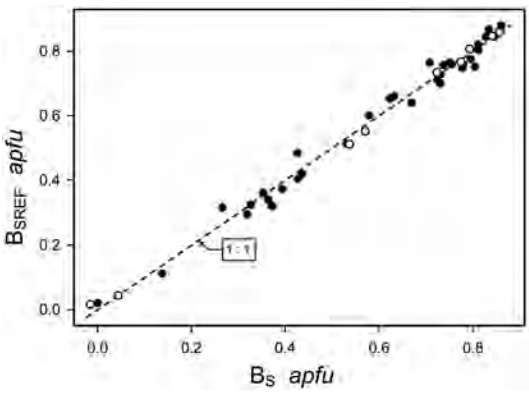

FIG. 2. Agreement between the observed (B_{SREF}) and calculated (B_S) B content (*apfu*) for the suite of kornerupine samples of Cooper *et al.* (2009a). B_S was calculated using equation (1), Table 1. White circles: nine samples for which X-ray powder-diffraction data were also collected. Dashed line is a 1:1 reference line.

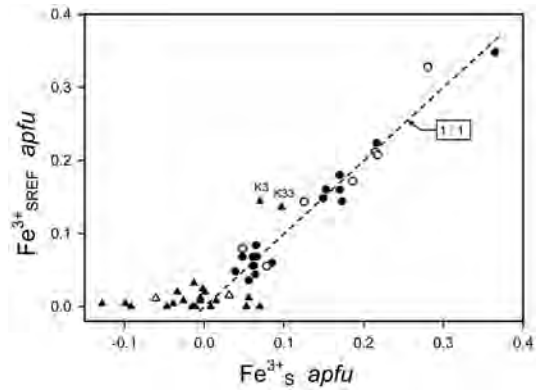

FIG. 3. Agreement between the observed (Fe^{3+}_{SREF}) and calculated (Fe^{3+}_S) Fe^{3+} content (*apfu*) for the suite of kornerupine samples of Cooper *et al.* (2009a). Fe^{3+}_S was calculated using equation (4), Table 1. Triangles: samples excluded from multiple regression with $Fe^{3+}_{SREF} \leq 0.03$ *apfu*. Circles: samples used for multiple regression with $Fe^{3+}_{SREF} > 0.03$ *apfu*. White symbols: nine samples for which X-ray powder-diffraction data were also collected. Dashed line is a 1:1 reference line.

TABLE 1. REGRESSION EQUATIONS INVOLVING CELL DIMENSIONS AND SELECTED CHEMICAL PARAMETERS OF THE KORNERUPINE STRUCTURE

(1)	$^{**}B_S = 62.5741 - 1.9758\ a_S - 4.4133\ c_S - 0.0189\ Al_2O_3 + 0.0089\ FeO^*$	$r^2 = 0.989$
(2)	$^{**}B_P = 62.5741 - 1.9758\ a_P - 4.4133\ c_P - 0.0189\ Al_2O_3 + 0.0089\ FeO^*$	–
(3)	$_cB_P = -[B_P * (-0.1548) + 0.04545] + B_P = 1.1548\ B_p - 0.04545$	
(4)	$Fe^{3+}_S = 3.1167 - 0.6303\ B_S - 0.0645\ Al_2O_3 + 0.0131\ FeO^*$	$r^2 = 0.952$
(5)	$Fe^{3+}_P = 3.1167 - 0.6303\ {}_cB_P - 0.0645\ Al_2O_3 + 0.0131\ FeO^*$	–

* all Fe expressed as FeO; ** S and P subscripts refer to single-crystal and powder-diffraction cell parameters, respectively.

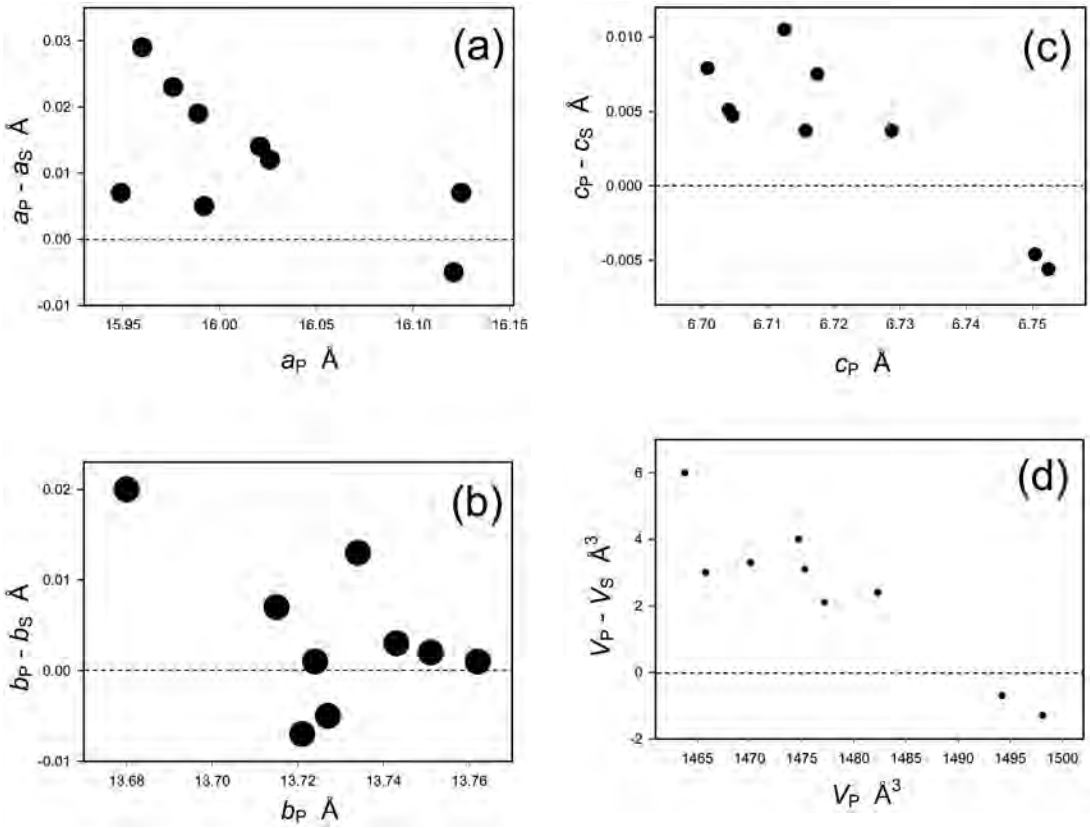

FIG. 4. Variation in the difference between cell parameters determined by single-crystal diffraction (subscript S) and powder diffraction (subscript P); (a) *a* cell parameter, (b) *b* cell parameter, (c) *c* cell parameter, (d) cell volume. Datapoint diameters are equal to twice the mean standard error for the refined powder-diffraction result.

can be universally indexed in an unambiguous manner with negligible interference from neighboring peaks (*i.e.*, with minimal systematic error). Least-squares refinement gave the cell parameters listed in Table 3.

The nine datapoints denoted by white circles on Figures 2 and 3 are from samples for which cell parameters were also calculated from X-ray powder data as part of this study. The differences in cell parameters refined by X-ray powder and single-crystal methods are shown as a function of the corresponding cell parameter from the powder method (Fig. 4). For each of the plots in Figure 4, the majority of the data fall above the dashed reference line at y = 0, indicating that the powder method generally gives larger unit-cell parameters than the single-crystal method. There is also a pronounced negative slope to the data points in the plots; this is best developed for the cell volumes (Fig. 4d). There is a systematic difference in the refined cell-parameters from single-crystal and powder methods, and therefore equation 2 (Table 1) should not be used alone to calculate a B content using cell parameters from powder-diffraction data.

TABLE 2. RECOMMENDED REFLECTIONS FOR USE IN LEAST-SQUARES REFINEMENT OF THE CELL DIMENSIONS OF KORNERUPINE FROM X-RAY POWDER-DIFFRACTION DATA

h k l	*d* range (Å)	*h k l*	*d* range (Å)
0 4 0	3.42–3.44	5 5 0	2.08–2.09
0 0 2	3.35–3.37	0 4 3	1.87–1.88
0 2 2	3.01–3.03	0 0 4	1.68–1.69
5 3 0	2.62–2.64	6 6 2	1.54–1.55
0 4 2	2.39–2.41	5 7 2	1.49–1.50
6 4 0	2.10–2.12		

PREDICTION OF B AND Fe^{3+}

Figure 5 shows the difference between the calculated B_P [equation (2) using powder-diffraction cell-parameters] and B_{SREF} *versus* the calculated B_P. At greater

TABLE 3. REFINED UNIT-CELL PARAMETERS FOR SELECTED SAMPLES OF KORNERUPINE

	K2	K6	K8	K16	K17	K25	K32	K36	K40
					*Single crystal**				
a (Å)	16.014(4)	15.970(6)	16.007(4)	15.931(5)	15.987(5)	15.953(3)	15.942(2)	16.125(2)	16.118(2)
b	13.728(2)	13.721(3)	13.749(3)	13.660(5)	13.740(3)	13.723(2)	13.708(2)	13.761(2)	13.732(2)
c	6.710(1)	6.712(2)	6.725(1)	6.699(2)	6.702(2)	6.700(1)	6.693(1)	6.758(1)	6.755(1)
V (Å^3)	1475.1(5)	1470.7(7)	1475.1(5)	1457.8(8)	1472.2(7)	1466.8(4)	1462.8(4)	1499.4(3)	1494.9(3)
					Powder				
a (Å)	16.026(4)	15.989(5)	16.021(5)	15.960(3)	15.992(5)	15.976(5)	15.949(4)	16.121(6)	16.125(5)
b	13.721(3)	13.734(3)	13.751(3)	13.680(2)	13.743(3)	13.724(4)	13.715(3)	13.762(4)	13.727(3)
c	6.7175(8)	6.7157(8)	6.7287(9)	6.7041(5)	6.7125(10)	6.7047(10)	6.7009(8)	6.7524(11)	6.7504(9)
V (Å^3)	1477.2(3)	1474.7(3)	1482.3(4)	1463.8(2)	1475.3(4)	1470.1(4)	1465.8(3)	1498.1(4)	1494.2(3)

*from Cooper *et al.* (2009a).

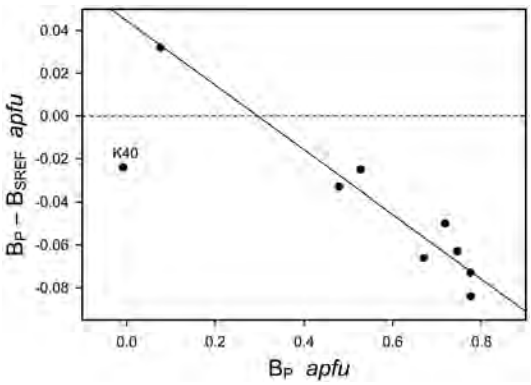

FIG. 5. Variation in the difference B_P–B_{SREF} and B_P. Solid line is a least-squares line through the data (excluding K40).

B content, the B calculated using powder-diffraction cell-parameters (B_P) is underestimated (by up to 10%) relative to the known B content (B_{SREF}). The solid line is a least-squares line through the data (excluding K40). A corrected content of B [$_CB_P$] can be calculated using equation (3). The various B values calculated using equations (1), (2) and (3) are compared to the B values from single-crystal structure refinement (B_{SREF}) in Table 4. For the nine samples studied by powder-diffraction methods, the final corrected B values [$_CB_P$] are in very close agreement with the B_{SREF} values.

Figure 5 also shows that the data point for K40 lies substantially off the regression line. Two possible factors may explain this: (1) the material for single-crystal and powder diffraction for K40 were from a large (15 cm) rock sample, and the relative sample locations and sample homogeneity are unknown; (2) of the kornerupine crystals studied, K40 has the lowest B content, and there may be other secondary crystal-chemical influences on the cell parameters in addition to those induced by a near-zero B content.

The values for B and Fe^{3+} calculated using the cell dimensions determined by X-ray powder diffraction are compared with the experimental values of B and Fe^{3+} (determined by SREF) in Figure 6. As is apparent from Figure 6, equations (3) and (5) (Table 1) accurately predict the B and Fe^{3+} contents of kornerupine.

SUMMARY

Carefully acquired X-ray powder data from clean separates of kornerupine will give accurate cell parameters *a*, *c*, and routine electron-microprobe analysis can provide accurate F, Al_2O_3 and FeO* contents. The H content is calculated using H = (1.0 – F), and the B and Fe^{3+} content can be calculated to within 0.05 *apfu* using the equations in Table 1. We hope that this procedure will lead to increased information and understanding concerning chemical variation in kornerupine as a function of paragenesis.

ACKNOWLEDGEMENTS

We thank Gianni Andreozzi and Sergio Lucchesi for their helpful comments on this manuscript. FCH was supported by a Canada Research Chair in Crystallography and Mineralogy, by Major Facilities Access, Research Tools and Equipment, and Discovery Grants from the Natural Sciences and Engineering Research Council of Canada, and by Innovation Grants from the Canadian Foundation for Innovation.

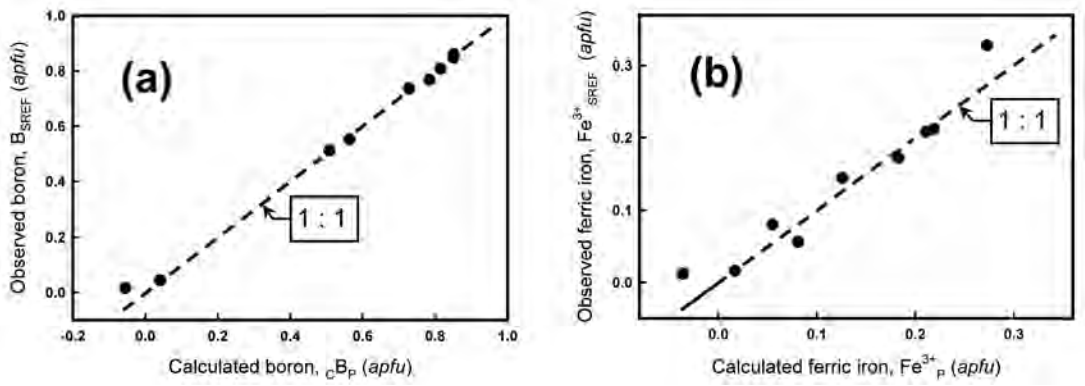

FIG. 6. Comparison of observed (subscript SREF) and calculated (subscript P, calculated from equations (3) and (5), Table 1]; (a) B and (b) Fe^{3+} in kornerupine. Dashed lines are 1:1 reference lines.

TABLE 4. SELECTED KORNERUPINE SAMPLES: Al_2O_3 and FeO* CONTENTS (wt.%), TOGETHER WITH OBSERVED (SREF) AND CALCULATED VALUES FOR B AND Fe^{3+} (*apfu*)

	K2	K6	K8	K16	K17	K25	K32	K36	K40
Al_2O_3	42.98	40.40	41.36	40.98	38.57	38.79	40.66	46.90	49.57
FeO*	3.02	9.83	9.40	10.84	10.44	9.93	2.63	4.47	0.57
B_{SREF}	0.512	0.736	0.552	0.860	0.768	0.848	0.808	0.044	0.016
B_S	0.536	0.723	0.571	0.856	0.774	0.841	0.793	0.044	–0.015
B_P	0.479	0.670	0.527	0.776	0.718	0.775	0.745	0.076	–0.008
$_CB_P$	0.508	0.728	0.563	0.851	0.784	0.850	0.815	0.042	–0.055
Fe^{3+}_{SREF}	0.080	0.172	0.212	0.056	0.328	0.208	0.016	0.144	0.012
Fe^{3+}_S	0.048	0.186	0.214	0.078	0.280	0.217	0.031	0.125	–0.061
Fe^{3+}_P	0.066	0.183	0.219	0.081	0.273	0.211	0.017	0.126	–0.036

* FeO*: all Fe expressed as FeO.

REFERENCES

COOPER, M.A., HAWTHORNE, F.C. & GREW, E.S. (2009a): The crystal chemistry of the kornerupine–prismatine series. I. Crystal structure and site populations. *Can. Mineral.* **47**, 233-262.

COOPER, M.A., HAWTHORNE, F.C., GREW, E.S. & ROSSMAN, G.R. (2009b): The crystal chemistry of the kornerupine–prismatine series. II. The role of hydrogen. *Can. Mineral.* **47**, 263-274.

GREW, E.S., CHERNOSKY, J.V., WERDING, G., ABRAHAM, K., MARQUEZ, N. & HINTHORNE, J.R. (1990): Chemistry of kornerupine and associated minerals, a wet chemical, ion microprobe and X-ray study emphasizing Li, Be, B and F contents. *J. Petrol.* **31**, 1025-1070.

HAWTHORNE, F.C., COOPER, M., BOTTAZI, P., OTTOLINI, L., ERCIT, T.S. & GREW, E.S. (1995): Microanalysis of minerals for boron by SREF, SIMS and SMPA: a comparative study. *Can. Mineral.* **33**, 389-397.

HAWTHORNE, F.C., COOPER, M.A. & GREW, E.S. (2009): The crystal chemistry of the kornerupine–prismatine series. III. Chemical relations. *Can. Mineral.* **47**, 275-296.

Received March 16, 2006, revised manusrcipt accepted April 3, 2009.